# What are the spins of stellar-mass black holes?

Andrzej Zdziarski
Centrum Astronomiczne im. M. Kopernika
Warszawa, Poland

# The GW-inferred effective and individual spins are very low

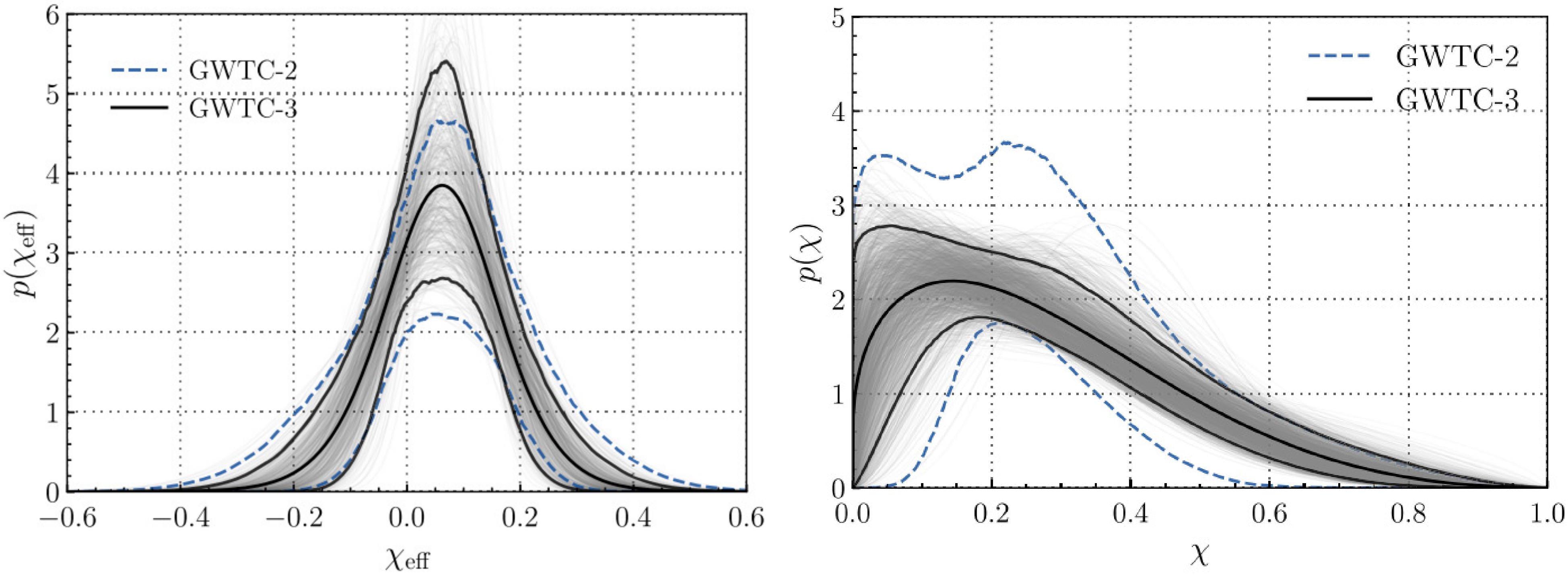


The Gravitational-Wave Transient Catalog 3 (GWTC-3), 70 binary BH mergers;
LVK collaboration 2023

# Large BH spins measured in X-ray binaries

| Source | Spin | Inclination [°] | Previous Spin | Previous Inclination [°] | Reference |
|---|---|---|---|---|---|
| AT 2019wey | $0.906^{+0.084}_{-0.202}$ | $14^{+12}_{-10}$ | $0.97^{+0.02}_{-0.03}$ | $22.0^{+2.6}_{-2.9}$ | Feng et al. (2022b) |
| LMC X-3 | $0.928^{+0.058}_{-0.146}$ | $38^{+14}_{-13}$ | $0.24 \pm 0.05^{\ddagger}$ | $69.24^{*}$ | Jana et al. (2021a) |
| LMC X-1 | $0.897^{+0.077}_{-0.176}$ | $50^{+10}_{-13}$ | $0.9395 \pm 0.015$ | $36.38^{*}$ | Jana et al. (2021a) |
| MAXI J0637-430 | $0.984^{+0.012}_{-0.042}$ | $63^{+9}_{-10}$ | $0.97 \pm 0.02$ | $62^{+3}_{-4}$ | Draghis et al. (2023b) |
| MAXI J1348-630 | $0.977^{+0.017}_{-0.055}$ | $52^{+8}_{-11}$ | $0.78 \pm 0.04$ | $29.2^{+0.3}_{-0.5}$ | Jia et al. (2022) |
| GS 1354-645 | $0.849^{+0.103}_{-0.221}$ | $47^{+11}_{-10}$ | $\geq 0.98$ | $75 \pm 2$ | El-Batal et al. (2016) |
| MAXI J1535-571 | $0.979^{+0.015}_{-0.049}$ | $44^{+17}_{-19}$ | $0.985^{+0.002}_{-0.004}$ | $72 \pm 2$ | Dong et al. (2022) |
| 4U 1543-47 | $0.959^{+0.031}_{-0.079}$ | $67^{+7}_{-8}$ | $0.98^{+0.01}_{-0.02}$ | $68^{+3}_{-4}$ | Draghis et al. (2023b) |
| MAXI J1631-479 | $0.951^{+0.039}_{-0.077}$ | $22^{+10}_{-12}$ | $\geq 0.94$ | $29 \pm 1$ | Xu et al. (2020) |
| 4U 1630-472 | $0.857^{+0.095}_{-0.211}$ | $55^{+8}_{-11}$ | $0.985^{+0.005}_{-0.014}$ | $64^{+2}_{-3}$ | King et al. (2014) |
| Swift J1658.2-4242 | $0.951^{+0.031}_{-0.069}$ | $50^{+9}_{-10}$ | $\geq 0.96$ | $64^{+2}_{-3}$ | Xu et al. (2018) |
| GX 339-4 | $0.97^{+0.026}_{-0.076}$ | $49 \pm 14$ | $0.95^{+0.02}_{-0.08}$ | $30 \pm 1$ | Parker et al. (2016) |
| IGR J17091-3624 | $0.963^{+0.027}_{-0.085}$ | $47^{+10}_{-11}$ | $0.07 \pm 0.2$ | $45.3 \pm 0.7$ | Wang et al. (2018b) |
| GRS 1716-249 | $0.97^{+0.022}_{-0.06}$ | $59^{+7}_{-12}$ | $\geq 0.92$ | $49.9^{+1.0}_{-1.3}$ | Tao et al. (2019) |
| MAXI J1727-203 | $0.962^{+0.034}_{-0.414}$ | $65^{+11}_{-14}$ | $0.986^{+0.012}_{-0.159}$ | $64^{+10}_{-7}$ | Draghis et al. (2023b) |
| Swift J1728.9-3613 | $0.868^{+0.058}_{-0.088}$ | $7^{+8}_{-3}$ | $0.86 \pm 0.02$ | $3.5^{+6.2}_{-0.5}$ | Draghis et al. (2023c) |
| GRS 1739-278 | $0.968^{+0.022}_{-0.074}$ | $70^{+5}_{-11}$ | $0.8 \pm 0.2$ | $43.2 \pm 0.5$ | Miller et al. (2015) |
| 1E 1740.7-2942 | $0.856^{+0.134}_{-0.443}$ | $31^{+29}_{-18}$ | $\geq 0.5$ | $63.7^{+4.6}_{-7.9}$ | Stecchini et al. (2020) |
| IGR J17454-2919 | $0.932^{+0.06}_{-0.363}$ | $54^{+15}_{-14}$ | $0.97^{+0.03}_{-0.17}$ | $60^{+8}_{-14}$ | Draghis et al. (2023b) |
| Swift J174540.2-290037 | $0.774^{+0.082}_{-0.106}$ | $31^{+8}_{-9}$ | $0.92^{+0.05}_{-0.07}$ | $21^{+2}_{-3}$ | Mori et al. (2019) |
| Swift J174540.7-290015 | $0.884^{+0.068}_{-0.109}$ | $63^{+10}_{-8}$ | $0.94^{+0.03}_{-0.1}$ | $64.2^{+0.9}_{-1.6}$ | Mori et al. (2019) |
| H 1743-322 | $0.949^{+0.039}_{-0.127}$ | $54^{+12}_{-13}$ | $0.98^{+0.01}_{-0.02}$ | $56 \pm 4$ | Draghis et al. (2023b) |
| Swift J1753.5-0127 | $0.989^{+0.007}_{-0.035}$ | $73 \pm 8$ | $0.997^{+0.001}_{-0.003}$ | $74 \pm 3$ | Draghis et al. (2023b) |
| GRS 1758-258 | $0.98^{+0.014}_{-0.058}$ | $67^{+8}_{-13}$ | $0.991^{+0.007}_{-0.019}$ | $66^{+8}_{-5}$ | Draghis et al. (2023b) |
| MAXI J1803-298 | $0.987^{+0.007}_{-0.037}$ | $72^{+6}_{-9}$ | $0.991 \pm 0.001$ | $70.8 \pm 1.1$ | Feng et al. (2022a) |
| MAXI J1813-095 | $0.88^{+0.1}_{-0.27}$ | $42^{+11}_{-13}$ | $\geq 0.76$ | $36.5 \pm 8.5$ | Jana et al. (2021b) |
| V4641 Sgr | $0.701^{+0.211}_{-0.272}$ | $66^{+7}_{-11}$ | $0.86^{+0.04}_{-0.06}$ | $66^{+3}_{-4}$ | Draghis et al. (2023b) |
| MAXI J1820+070 | $0.967^{+0.025}_{-0.061}$ | $64^{+8}_{-9}$ | $0.988^{+0.006}_{-0.028}$ | $64^{+3}_{-4}$ | Draghis et al. (2023b) |
| MAXI J1848-015 | $0.753^{+0.191}_{-0.652}$ | $29^{+13}_{-10}$ | $0.967 \pm 0.013$ | $26.4 \pm 0.5$ | Pike et al. (2022) |
| EXO 1846-031 | $0.959^{+0.031}_{-0.077}$ | $62^{+9}_{-10}$ | $0.997^{+0.001}_{-0.002}$ | $73^{+2}_{-1}$ | Draghis et al. (2020) |
| XTE J1908+094 | $0.466^{+0.368}_{-0.517}$ | $28 \pm 11$ | $0.55^{+0.29}_{-0.45}$ | $27^{+2}_{-3}$ | Draghis et al. (2021) |
| GRS 1915+105 | $0.976^{+0.018}_{-0.056}$ | $60 \pm 8$ | $0.98 \pm 0.01$ | $72 \pm 1$ | Miller et al. (2013) |
| Cyg X-1 | $0.95^{+0.04}_{-0.084}$ | $47^{+9}_{-11}$ | $\geq 0.97$ | $45.3 \pm 0.4$ | Parker et al. (2015) |
| 4U 1957+11 | $0.9^{+0.08}_{-0.28}$ | $52^{+12}_{-13}$ | $0.95^{+0.02}_{-0.04}$ | $52^{+4}_{-5}$ | Draghis et al. (2023b) |
| XTE J2012+381† | $0.988^{+0.008}_{-0.03}$ | $68^{+6}_{-11}$ | ... | ... | Draghis et al. (2023a) |
| V404 Cyg | $0.935^{+0.037}_{-0.075}$ | $37^{+9}_{-8}$ | $\geq 0.92$ | $52^{+2}_{-3}$ | Walton et al. (2017) |

Draghis+24

# A new disk model modification: warm disk coronae

- Warm disk layers, Comptonizing the underlying disk emission, have been widely considered to explain soft X-ray excesses in AGNs (e.g., Magdziarz+98; Petrucci+20; Ursini+20; Xiang+22; Ballantyne+24).
- The parameters of the Comptonizing layers are typically $kT_{\rm e} \sim 1$ keV and the Thomson optical depth of $\tau_{\rm T} \gg 1$.

# Spectral fits for Cyg X-1 – low spin with a warm corona

NICER+NuSTAR+INTEGRAL

$a_* = 0.87^{+0.04}_{-0.03}$ $a_* = 0.00^{+0.07}$

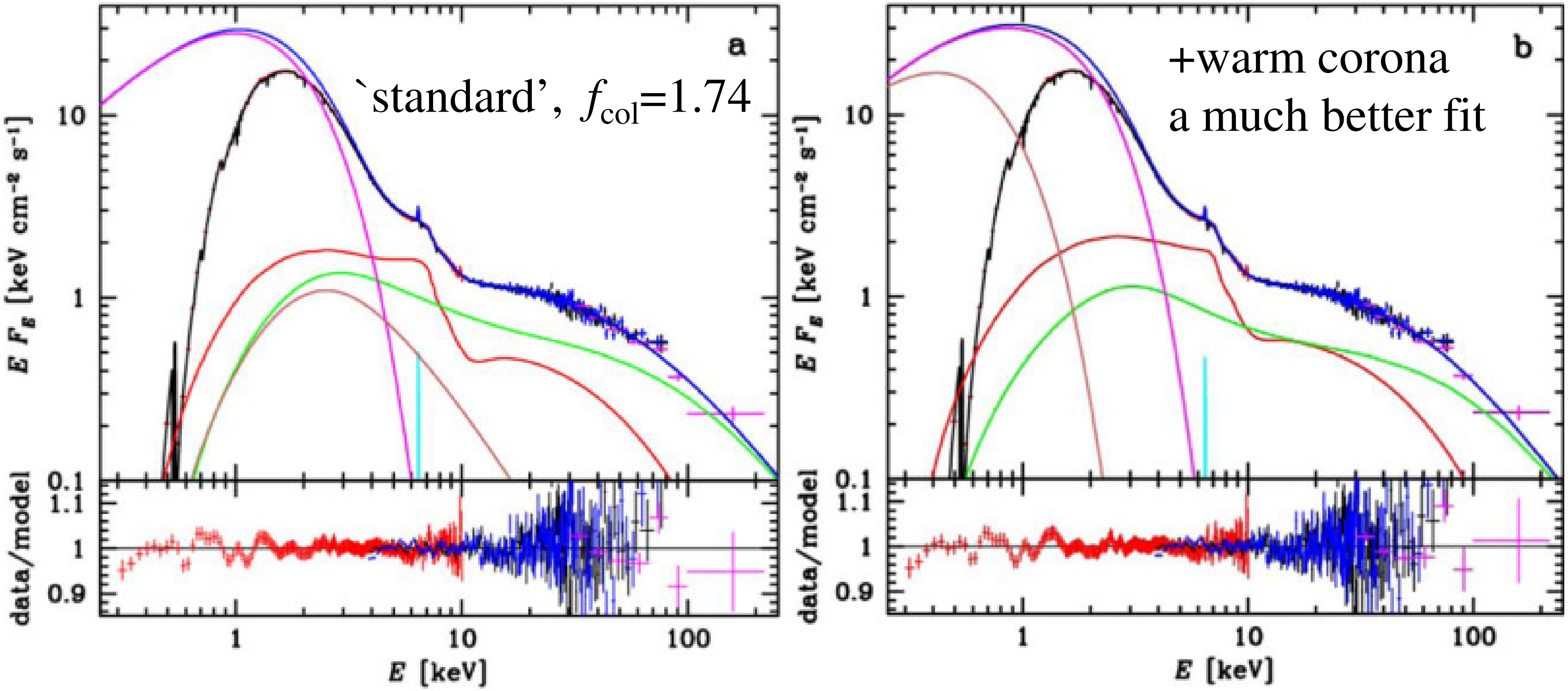


$\chi^2_\nu$ =741/607 $\chi^2_\nu$=705/605